JOC The Journal of Organic Chemistry

Article

pubs.acs.org/joc

Long-Wavelength, Photostable, Two-Photon Excitable BODIPY Fluorophores Readily Modifiable for Molecular Probes

Xinfu Zhang,[†] Yi Xiao,*[,†] Jing Qi,[‡] Junle Qu,*[,‡] Bosung Kim,[§] Xiling Yue,[§] and Kevin D. Belfield*[,§]

[†]State Key Laboratory of Fine Chemicals, Dalian University of Technology, 2 Linggong Road, Dalian 116024, People's Republic of China

[‡]Key Laboratory of Optoelectronic Devices and Systems of Ministry of Education and Guangdong Province, College of Optoelectronic Engineering, Shenzhen University, Nanhai Road 3688, Shenzhen 518060, People's Republic of China

[§]Department of Chemistry and CREOL, College of Optics and Photonics, University of Central Florida, P.O. Box 162366, Orlando, Florida 32816-2366, United States

Supporting Information

ABSTRACT: Near-infrared (NIR) fluorescent probes are increasingly popular in biological imaging and sensing, as long-wavelength (650−900 nm) excitation and emission have the advantages of minimum photodamage, deep tissue penetration, and minimum interference from autofluorescence in living systems. Here, a series of long-wavelength BODIPY dyes **SPC**, **DC-SPC**, **DPC**, and **DC-DPC** are synthesized conveniently and efficiently. They exhibit excellent photophysical properties in far red to near-infrared region, including large extinction coefficients, high fluorescence quantum yields, good photostability, and reasonable two-photon absorption cross section. Comparison of single-molecular imaging confirms that **DPC** is a much more efficient and more photostable NIR fluorophore than the commonly used **Cy5**. Also importantly, two kinds of convenient functionalization sites have been reserved: the aryl iodide for organometallic couplings and the terminal alkyne groups for click reactions. Further derivatives **DC-SPC-PPh3** exhibit specificity to localize in mitochondria. The introduction of triphenylphosphonium (TPP) moieties mediates its hydrophilic−lipophilic balance and makes **DC-SPC-PPh3** appropriate for cell labeling. Their long-wavelength emission at ∼650 nm can efficiently avoid the spectral crosstalk with other probes emitting in the visible light region. Superior photostability, low cytotoxicity, and two-photon excitable properties demonstrate its utility as a standard colocalizing agent to estimate the other probes' local distribution.

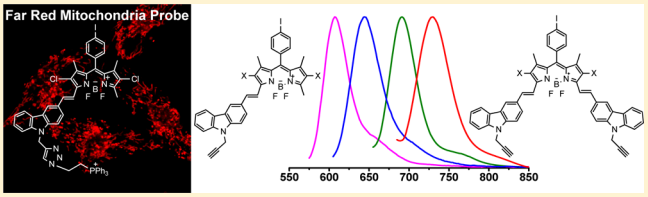

INTRODUCTION

Near-infrared (NIR) fluorescent probes are increasingly popular in biological imaging and sensing, as long-wavelength (650−900 nm) excitation and emission have the advantages of minimum photodamage to biological samples, deep tissue penetration, and minimum interference from background autofluorescence by biomolecules in the living systems.[1] However, as compared to the large amount and widespread use of the probes in the UV−visble region, the number of NIR probes is limited, and their practical applicability needs to be further improved.

The development of NIR fluorescent probes encounters bottlenecks produced by the lack of appropriate fluorophores. Up to now, the only common NIR fluorophores belong to cyanine dyes, such as **Cy5** and **Cy7**.[2] Yet their photostabilities are unsatisfactory, and their fluorescence quantum yields are suboptimal.[3] Especially in real time imaging of living cells or tissues, photostability is an important feature that defines fluorescence dyes. This situation urges a few research groups, including ours, to search for novel ones.[4−7] Recent examples include Si-rhodamines,[4] AZA-Bodipys,[5] Changsha NIRs,[6a] and squaraines,[6b] etc. Even though photophysical properties of these new NIR fluorophores are enhanced to some extent, most of them have complex structures and involve tanglesome synthetic methodologies, which make their further derivatization to obtain probes very difficult to achieve.

Currently, there is also an urgent demand to develop organelle-targetable NIR probes that can be separable from the fluorescence windows of other probes emitting in visible range. Subcellular organelle-specific probes provide an advantageous way to collect accurate local information from intracellular regions of interest. For this reason, a variety of organelle-specific probes are being explored.[8] Commercially available organelle-specific probes, such as the Mitotrackers that stain mitochondria specifically, and Lysotrackers that localize in lysosomes, have made the exploitation of other new specific probes easier, as they can act as colocalizing agents in cell imaging. Unfortunately, almost all of these commercial trackers have absorption and emission in the visible range (400−650 nm), which is also the spectrum range of most other fluorescent probes. Sometimes, spectral crosstalk is so serious that the colocalization becomes unreliable. Thus, new NIR organelle trackers will help in addressing this issue.

Received: June 25, 2013
Published: August 28, 2013

dx.doi.org/10.1021/jo401379g | J. Org. Chem. 2013, 78, 9153−9160

Scheme 1. Synthetic Procedures for SPC, DPC, DC-SPC, DC-DPC, DC-SPC-PPh3, and DC-DPC-PPh3[a]

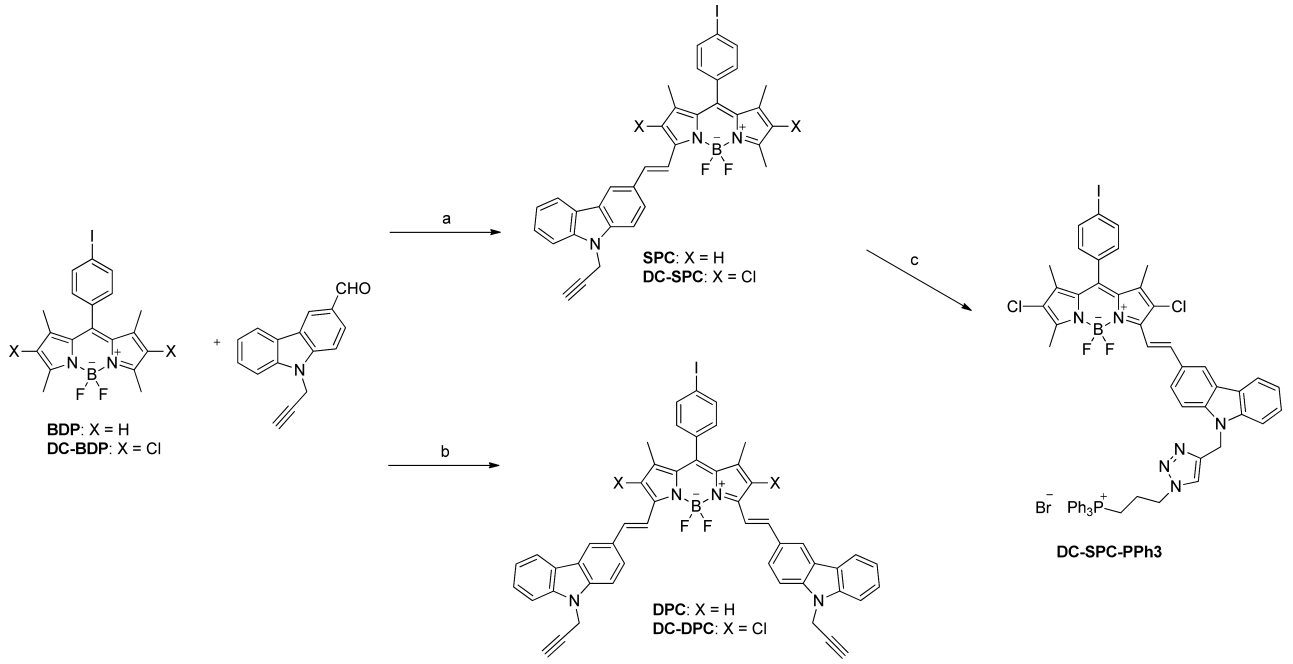

[a]Conditions: (a) Piperidine, acetic acid, toluene, reflux by using a Dean–Stark trap, 8 h. (b) Piperidine, acetic acid, anhydrous magnesium perchlorate, toluene, reflux by using a Dean–Stark trap, 8 h. (c) (3-Azidopropyl)-triphenylphosphonium bromide, **DIPEA**, $CuSO_4$, sodium ascorbate, alcohol, H_2O, toluene, rt, overnight.

In this Article, a series of new BODIPY (4,4-difluoro-4-bora-3*a*,4*a*-diaza-*s*-indacene) derivatives have been developed to overcome the problems during the development of NIR dyes (Scheme 1). These fluorophores emit intensive far red to near-infrared fluorescence, they are photostable, and importantly they are easily prepared. Besides, two kinds of convenient functionalization sites have been reserved: the aryl iodide for organometallic couplings and the propargyl groups for click reactions. By attaching one triphenylphosphonium (TPP) moiety to the above BODIPYs, we obtain a positively charged probe, which specifically localizes in mitochondria.

RESULTS AND DISCUSSION

Design and Synthesis of Long-Wavelength BODIPY Derivatives: SPC, DC-SPC, DPC, DC-DPC. Long-wavelength and convenient derivative approaches are mainly considered during the designing of these BODIPY dyes. Two strategies, extending π-conjugations[9] and forming moderate ICT (intramolecular charge Ttansfer)[10] structures, are general methods employed in designing long-wavelength dyes. The former usually results in long-wavelength derivatives that inherit the excellent optical properties from the BODIPY precursors, but in many cases it requires superb synthetic skills; for example, much research has fused aromatic or heterocyclic rings to the BODIPY core via relatively long synthetic routes.[11] The ICT strategy is very effective in producing red shifts and is relatively easy to realize in synthesis. However, the reported BODIPY derivatives of strong ICT character lose some of the typical characteristics of the family. In highly polar media, a significant decrease in fluorescence intensity and broadening in fluorescence spectra are observed.[10a,12] According to our previous work, introduction of the carbazole group to BODIPY core will optimize spectral properties.[13] It is a good choice that combines the above two strategies, because of its aromaticity and moderate ICT strength. On the other hand, the aryl iodide and the propargyl groups through carbazole are designed in BODIPY dyes. These dyes can be further functionalized through organometallic couplings or click reactions, which are important for NIR dyes to be applied.

As shown in Scheme 1, BODIPY dyes **SPC**, **DPC**, **DC-SPC**, and **DC-DPC** have been synthesized efficiently and in high yield by the classical Knoevenagel condensation of 3,5-dimethyl-BODIPY dyes with *N*-propargyl carbazole aldehyde. This strategy has been proven efficient to extending π-conjugations by the research works of Rurack, Akkaya, and Ziessel, etc.[7,9,10] Knoevenagel reaction on the 3- and 5-methyl sites is in most cases high yielding and can be carried out in large scale. Moreover, chlorines on 2,6-positions may increase the electron density of the carbon atoms on 3,5-positions and then increase the condensation reactivity.[14] Thus, two parent BODIPY dyes are used, one of which, **DC-BDP**, is chloro-substituent on the 2,6-positions. Knoevenagel condensation of **DC-BDP** proceeded more efficiently than that of **BDP**. In general, **DPC** and **DC-DPC**, the products of twice condensations, show satisfactory isolated yields of 75% and 80%, respectively. The monocondensations are also readily controllable by adjusting the mole ratio and stopping the reaction at a proper time to get **SPC** or **DC-SPC** with optimized yield of about 35%. Restricted by tanglesome synthetic methodologies, rarely any new NIR fluorescent dyes have been further applied in biomedical analysis. Here, provision of larger quantities will not be a bottleneck for further applications of these BODIPY dyes. **DC-SPC** is facilely functionalized via click chemistry into **DC-SPC-PPh3**, which possesses the enhanced solubility in polar solvents and maintains similar photophysical properties. The introduction of triphenylphosphonium (TPP) moieties mediates its hydrophilic–lipophilic balance and makes **DC-SPC-PPh3** appropriate for cell labeling. All imaging experi-

dx.doi.org/10.1021/jo401379g | J. Org. Chem. 2013, 78, 9153–9160

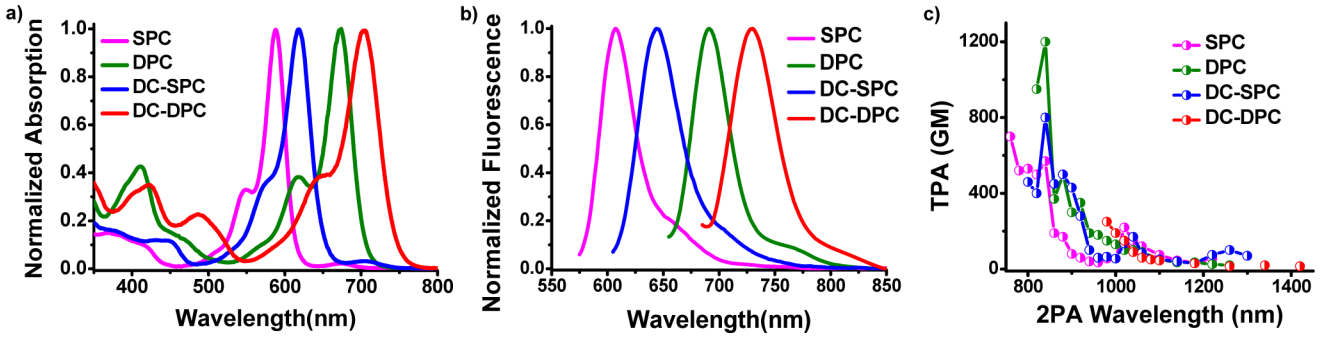

Figure 1. (a) Normalized absorption spectra, (b) normalized fluorescence spectra, and (c) two-photon absorption spectra of **SPC**, **DPC**, **DC-SPC**, and **DC-DPC** in chloroform.

Table 1. Photophysical Properties of SPC, DPC, DC-SPC, and DC-DPC

dyes	solvent	λ_{abs} (nm)	ε (M^{-1} cm^{-1})	λ_{em} (nm)	Φ_f	τ (ns)	K_r[c] (10^8 s^{-1})	K_{nr}[c] (10^8 s^{-1})	δ[d] (GM)
SPC	chloroform	588	124 200	607	0.66[a]	3.93	1.67	0.87	700 (760 nm)
	acetonitrile	579	120 800	605	0.77	4.03	1.91	0.57	nd
	DMSO	589	110 600	614	0.72	3.64	1.98	0.77	nd
DC-SPC	chloroform	619	92 800	644	0.62[a]	4.24	1.46	0.89	800 (840 nm)
	acetonitrile	606	92 100	650	0.43	3.95	1.09	1.44	nd
	DMSO	616	77 900	666	0.33	3.06	1.07	2.19	nd
DPC	chloroform	674	105 900	691	0.99[b]	4.00	2.48	0.02	1200 (840 nm)
	acetonitrile	665	99 600	688	0.96	4.14	2.32	0.10	nd
	DMSO	678	94 900	703	0.97	3.61	2.69	0.08	nd
DC-DPC	chloroform	703	86 100	730	0.55[b]	3.97	1.39	1.13	250 (980 nm)
	acetonitrile	694	68 600	731	0.50	3.94	1.27	1.27	nd
	DMSO	705	68 700	749	0.32	3.05	1.05	1.25	nd
DC-SPC-PPh3	EtOH	612	89 800	650	0.40[a]	nd	nd	nd	nd

[a]Rhodamine B is used as standard. [b]Reported 3,5-bi (*p*-methoxy) phenyl-1,7-bi (*p*-bromo) phenyl aza-BODIPY (Φ_f 0.42, in toluene) is used as standard. [c]Radiative (K_r) and nonradiative (K_{nr}) decay rates. [d]Maximum two-photon absorption cross section, 1 GM = 10^{-50} cm^4 s $photon^{-1}$.

ments are carried out following the regular operation without worrying about its solubility in biological media.

Fundamental Optical Properties and Photostability. These NIR dyes have been qualified for biological imaging by their outstanding optical characteristics. The normalized absorption and emission spectra in chloroform are recorded in Figure 1, and the spectra data are listed in Table 1. These BODIPY dyes exhibit strong emission in the far red to NIR region. After the introduction of chlorines and carbazole groups, the emission peak is pushed stepwise from about 500 to 614, 666, 703, and 749 nm. As compared to **SPC** and **DPC**, respectively, chlorides on 2,6-positions of **DC-SPC** and **DC-DPC** also cause a red shift of about 40 nm for both absorption and emission. Importantly, these four long-wavelength fluorophores have inherited the BODIPY family's excellent photophysical properties, such as high molar extinction coefficient (70 000−120 000 M^{-1} cm^{-1}), small fwhm (full width at half-maximum) of spectrum (37−48 nm), and high quantum yield (e.g., 0.55−0.99 in chloroform; 0.40−0.96 in acetonitrile). Also, noticeably, in highly polar solvents such as DMSO, their emission spectra shift slightly relative to those in chloroform, and fluorescence quantum yields remain high, which indicate that they are also environmental factor-independent fluorophores as typical BODIPYs.[15] This is totally different from some previous long-wavelength BODIPY derivatives of apparent ICT character.

Quantum yield is actually a result of competition between nonradiative deactivation processes and fluorescence emission.[5a] For better understanding this, fluorescence lifetimes (τ) of these dyes were measured. Their lifetimes are approximately 4 ns (Table 1). Further, both radiative (K_r) and nonradiative (K_{nr}) decay rates (in relation to Φ_f and τ) are calculated. The result shows that the weight of the radiative channel in the total decay is big enough, which means that these dyes emit intensely.

The two-photon absorption (2PA) spectra have been measured through the femtosecond Z-scan technique, as shown Figure 1c. These BODIPY dyes exhibit a reasonable 2PA cross section δ. Across the 760−1100 nm spectral window, **SPC**, **DC-SPC**, and **DPC** show maximum δ 700, 800, and 1200 GM at 760, 840, and 840 nm, respectively. Although the NIR dye **DC-DPC** only gives a moderate δ 250 GM at 980 nm, this might not be the real maximum, because its Z-scan is performed only in the 980−1400 nm range, to completely rule out the interference from the long-wavelength one-photon absorption.

Our fluorophores with combined two-photon excitation and long-wavelength emission will be very advantageous over those common used two-photon fluorophores emitting in the visible range and those common one-photon NIR emitters with poor two-photon activities. As is known, two-photon microscopy gains increasing popularity in biological imaging because of its considerable imaging depth inside intact tissues (>500 μm), inherent three-dimensional resolution without out-of-focus fluorescence, and the limited photobleaching and photodamage to the focal volume.[16] However, the relatively short-wavelength emission of the most known two-photon fluorophores tends to

dx.doi.org/10.1021/jo401379g | J. Org. Chem. 2013, 78, 9153−9160

be obscured in biological background fluorescence, which, to some extent, offsets the benefit of NIR two-photon excitation.

Photodecomposition experiments prove that these BODIPY dyes have good photostability. Here, photostabilities of these dyes has been compared to that of the well-known NIR fluorophore **Cy5** (Supporting Information Figure S7) in chloroform. These BODIPY dyes show superior photostability over **Cy5** (Figure 2). After irradiation by a 500 W iodine

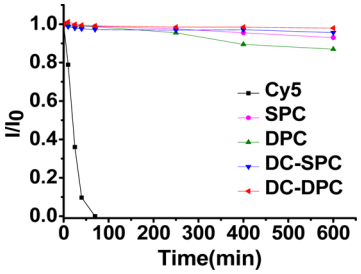

Figure 2. Fluorescence intensity decay of **SPC**, **DPC**, **DC-SPC**, **DC-DPC**, and **Cy5** in chroloform with irradiation by a 500 W iodine–tungsten lamp. I_0 is the fluorescence intensity immediately after the irradiation. I is the fluorescence intensity of the above compounds after a fixed time of irradiation.

tungsten lamp for 475 min, the fluorescence of these BODIPY dyes remains as high as 95%, while **Cy5** is totally bleached within 100 min. Enhanced photostability demonstrates the advantage of these NIR fluorescence dyes for bioapplications.

DFT Calculations. DFT calculations are carried out for further understanding of structure–property relationships,[17] with part of the data listed in Table 2. The small dihedral angles (less than 10°) between the numbered atoms demonstrate high planarity between the BODIPY core and carbazole group (Figure 3A and Supporting Information Figure S5). In addition, the HOMO and LUMO electron distribution of **DC-DPC** illustrates the transition dipole moment is larger than a typical $\pi-\pi^*$ transition (Figure 3B and Supporting Information Figure S5). The above two results are in accordance with our designing strategies: extending π-conjugations and forming moderate ICT. Moreover, HOMO and LUMO data show that the introduction of carbazole group will raise the HOMO energy level pronouncedly, and the introduction of chlorine will drop the LUMO energy level. It means smaller energy transitions and bathochromic shifts for **SPC**, **DC-SPC**, **DPC**, and **DC-DPC** as compared to **BDP**. Calculated absorption shows the general trend of red shift stepwise from 407 nm to 525, 565, 613, 654 nm, and these values are close to the experimental results. Another benefit from the quantum calculation is to estimate the lowest-lying singlet excited state, which is responsible for the emissive property of the fluorophore. According to the quantum mechanics selection

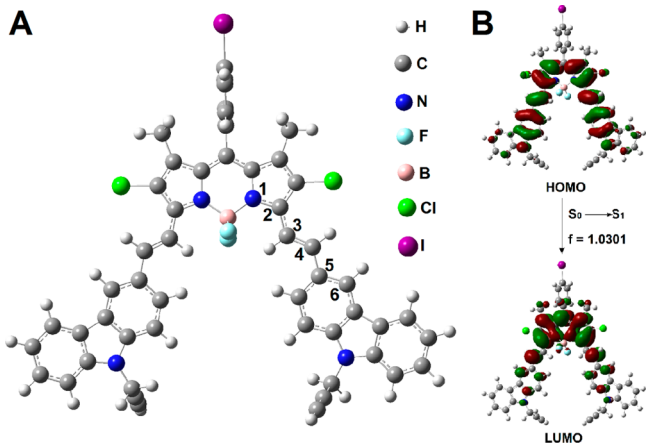

Figure 3. (A) DFT optimized structure of **DC-DPC** in the ball-and-stick representation. (B) The HOMO and LUMO electron distribution of **DC-DPC**.

rule, emissive property (as well as the excitation) of a dye can be evaluated by the symmetry and the overlapping of the molecular orbitals (MOs), the change of the spin state, and the oscillator strength (f) of the electronic transitions, etc.[18] The DFT calculation demonstrates these NIR dyes bear a higher $S_1 \leftarrow S_0$ transition oscillator strength (f) of more than 1. This means the reverse transition, that is, $S_1 \rightarrow S_0$ transition, is also fully allowed; thus, this dye is potentially fluorescent. These results are in good agreement with the experimental quantum yield.

Single-Molecule Experiment. Single-molecule imaging investigation also confirms **DPC** to be a very efficient and photostable NIR emitter. As the representative of these new BODIPYs, **DPC** is chosen for the comparison with **Cy5**, because they have similar absorption and emission wavelengths. Single-molecule imaging experiments are performed in PMMA (Figure 4). This is a standard test of a fluorophore to be used in imaging at single-molecule level, which requires bright fluorescence and robust photostability.[19] Typical time (Figure 4C) traces of single-molecule **DPC** and **Cy5** illustrate that, in most cases, **DPC** single molecule exhibits longer surviving time (approximate 100 slides = 5000 ms) and higher emission rate (approximate 45 000 photons per 50 ms). Hence, the total number of collected photons before bleaching of **DPC** will be much larger than that of **Cy5** (about 4 times simply by integral area). Considering the long wavelength, as well as large two-photon action cross section and good photostability in both bulk and single-molecule state, **DPC** exhibits obvious superiority over **Cy5** as a NIR fluorophore.

Mitochondrial Targetable Fluorescent Probe and Its Application for Biological Imaging. **DC-SPC-PPh3** is then qualified as a useful mitochondrion tracker in both one-photon

Table 2. DFT Calculation Results[a]

dyes	$\varphi_{C1-C2-C3-C4}$[b]	$\varphi_{C3-C4-C5-C6}$[b]	energy (eV)[c]	f[d]	HOMO/LUMO (eV)
BDP			3.05 (407 nm)	0.4493	−5.61/−2.61
SPC	6.99	0.84	2.36 (525 nm)	1.2179	−4.98/−2.58
DC-SPC	9.56	0.90	2.19 (565 nm)	1.0939	−5.22/−2.97
DPC	5.26	1.10	2.02 (613 nm)	1.2271	−4.68/−2.59
DC-DPC	2.82	1.84	1.89 (654 nm)	1.0301	−4.90/−2.91

[a]Calculations were carried out using the Gaussian 09 programs, employing the B3LYP functional. [b]φ stands for dihedral angle between the numbered atoms. [c]Optical band gap and calculated absorption wavelength. [d]Oscillator strength of $S_1 \leftarrow S_0$ transition.

dx.doi.org/10.1021/jo401379g | J. Org. Chem. 2013, 78, 9153–9160

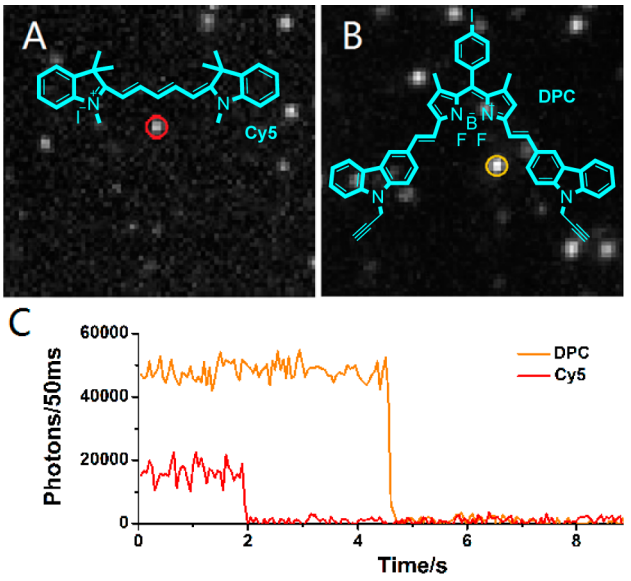

Figure 4. Single-molecule imaging of a PMMA film containing **Cy5** (A) and **DPC**, respectively. (B) The excitation wavelength is 656 nm, and laser intensity at the sample is approximate 0.25 kW/cm^2. (C) The spatially integrated fluorescence intensity time traces of the representative individual molecule, red for **Cy5** and orange for **DPC**. The reported intensity is background-subtracted. Because of photobleaching, the emission terminates at 2 and 4.5 s for **Cy5** and **DPC**, respectively.

and two-photon imaging experiments. Colocalization study of **DC-SPC-PPh3** with Rh-123 (commercial mitochondrial probe) has been conducted. As demonstrated in Figure 5, fluorescence intensity profiles of linear region of interest (ROI) across MCF-7 cells stained with **DC-SPC-PPh3** and Rh-123 vary in close synchrony (Figure 5D). Pearson's coefficient and overlap coefficient are 0.863 and 0.887, respectively, evaluated using the conventional dye-overlay method (Supporting Information Figure S6). Moreover, two-photon fluorescence images are collected to demonstrate the advantage of using **DC-SPC-PPh3** as a mitochondrial probe for 2PFM imaging. In Figure 6, the two-photon fluorescence image of MCF-7 cells is identical to the one-photon image. According to pioneering works of Chang and others,[20] the mitochondrial targetability of **DC-SPC-PPh3** should be ascribed to the positively charged alkyltriphenylphosphonium (TPP) moiety.

In Vivo Photodecomposition Experiments. In vivo photodecomposition experiments also reveal that **DP-SPC-PPh3** has much better photostability than widely used mitochondrial probes, such as Rh-123 and TMRM. After irradiation by semiconductor laser (488 nm for Rh-123, 559 nm for TMRM and **DC-SPC-PPh3**, 0.5 mW) on a confocal fluorescence microscope for 140 s, the fluorescence of **DC-SPC-PPh3** remains as high as 88%, while the other two show obvious decreases, TMRM to 30% and Rh123 to 9% (Figure 7). Photodecomposition experiments are also conducted by using 2PM. After irradiation by 800 nm (1 mW) for 140 s, the fluorescence of **DC-SPC-PPh3** remains as high as 72%. Rh123 and TMRM show equally high photostability against two-photon excitation at 800 nm. However, it may be because the latter two dyes bear a smaller two-photon absorption cross section. Enhanced photostability demonstrates the advantage of **DC-SPC-PPh3** as a first choice far red mitochondrial tracker in living cells.

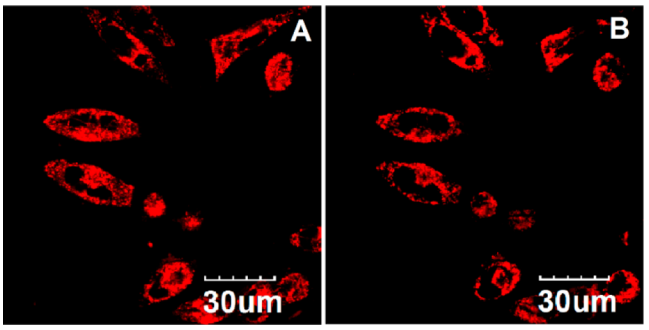

Figure 6. MCF-7 cells are costained with 37.5 nM **DC-SPC-PPh3** (1 h at 37 °C, 5% CO_2) in PBS. (A) and (B) are OPM (λ_{ex} = 559 nm, λ_{em} = 600−660 nm, pseudocolor red) and 2PM (λ_{ex} = 900 nm, λ_{em} = 600−660 nm, pseudocolor red) images of MCF-7 cells stained by **DC-SPC-PPh3**.

Cytotoxicity Study. The cytotoxicity of **DC-SPC-PPh3** is low. MTT assay (Figure 8) has revealed that even incubated with a much higher concentration (10 μM) than the optimized level, ~95% of MCF-7 cells survive after 24 h. This is a favorable characteristic of a practical mitochondrial probe applied in living cells.

■ CONCLUSION

To develop efficient and photostable long-wavelength fluorescent probes, we have synthesized a series of BODIPY derivatives such as **SPC**, **DPC**, **DC-SPC**, and **DC-DPC** in high yields through Knoevenagel condensation. These dyes emit at tunable wavelengths in the far-red to NIR region; for example,

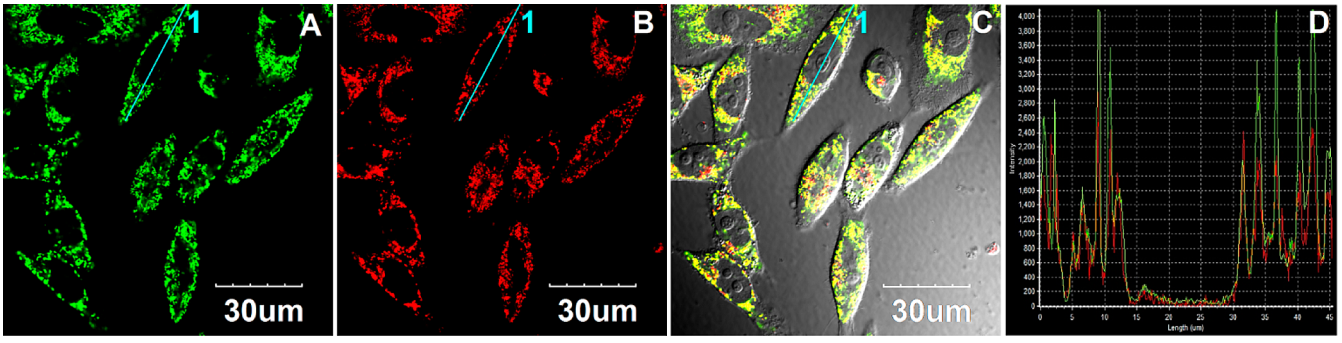

Figure 5. MCF-7 cells are costained with (A) 25 nM Rh-123 (λ_{ex} = 488 nm, λ_{em} = 500−560 nm, pseudocolor green) and (B) 37.5 nM **DC-SPC-PPh3** (λ_{ex} = 559 nm, λ_{em} = 600−660 nm, pseudocolor red) (1 h at 37 °C, 5% CO_2) in PBS. (C) Overlay of (A), (B), and brightfield. (D) Intensity profile of region of interest (ROI) cross MCF17 cell.

dx.doi.org/10.1021/jo401379g | J. Org. Chem. 2013, 78, 9153−9160

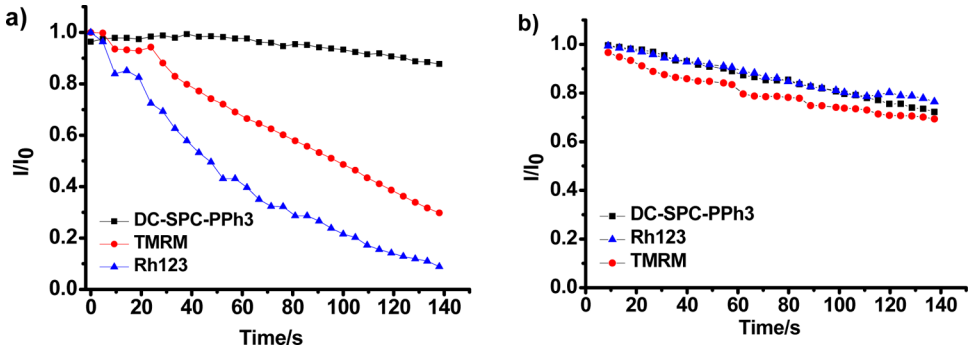

Figure 7. Photofading of dyes (**DC-SPC-PPh3**, Rh123, and TMRM) in living cells with irradiation by semiconductor laser in a confocal fluorescence microscope. (a) Excitation wavelength is 488 nm for Rh-123, 559 nm for TMRM and **DC-SPC-PPh3**, and the intensity at the sample is approximately 0.5 mW. (b) Excitation wavelength is 800 nm (2PM) for Rh-123, TMRM, and **DC-SPC-PPh3**, and the intensity at the sample is approximately 1 mW.

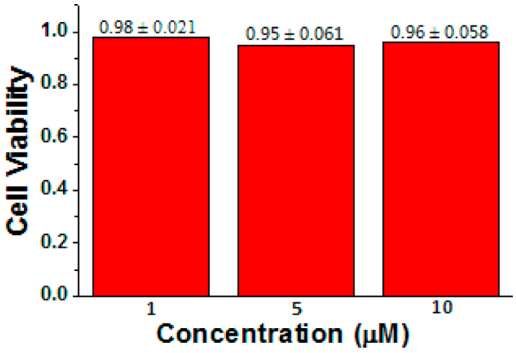

Figure 8. Viability of MCF-7 cells with **DC-SPC-PPh3** after treatment in different concentrations for 24 h.

in chloroform their emission peak is 607, 644, 691, and 730 nm, respectively. Importantly, their fluorescent quantum yields are very high, regardless of the solvents' polarity. For example, in chloroform, these values are up to 0.66, 0.62, 0.99, and 0.55, respectively. They are much more efficient and much more photostable emitters than common NIR dyes, for example, **Cy5**, as proved by the comparison study of single-molecule fluorescence imaging. Another advantage lies in that they have reasonable two-photon absorption across sections. These precursors bearing terminal acetylene groups are readily modified into organelle-targetable probes, for example, **DC-SPC-PPh3** via Click chemistry, while **DC-SPC-PPh3** exhibits specificity to localize in mitochondria in living cells. Because its long-wavelength emission at ~650 can efficiently avoid the spectral crosstalk with other probes emitting in the visible light region, **DC-SPC-PPh3** will act as standard colocalizing agent to estimate the other probes' local distribution in both OPM imaging and 2PM imaging. We expect that they will become valuable tools for fluorescent imaging and sensing in cell biology.

EXPERIMENTAL SECTION

Materials. Carbazole aldehydes, 3-nitrine propyl triphenylphosphonium, and DC-BDP are synthesized according to standard procedures.[1,2] Toluene is dried over suitable reagents and distilled under argon immediately prior to use. The commercial dyes **Cy5**, neutral red, and Rh-123 are used as received with a purity >99% (checked by spectroscopic and chromatographic methods). Solvents for spectra studies are of spectroscopic grade and are used without purification.

General Methods. The 400 (^{1}H) MHz NMR and 100 (^{13}C) MHz NMR spectra are registered at rt using perdeuterated solvents as internal standard. Melting points were obtained with a capillary melting point apparatus in open-ended capillaries and are uncorrected. Chromatographic purification is conducted with silica gel. All solvent mixtures are given as volume/volume ratios. The slit width is 3 nm for both excitation and emission during fluorescence spectra recording. Relative quantum efficiencies of fluorescence of compounds are obtained by comparing the areas under the corrected emission spectrum of the test sample in diluted solvents with that of Rhodamine B (Φ_F = 0.69) in methanol and a reported aza-BODIPY derivative in toluene, which has a quantum efficiency of 0.42 according to the literature.[3] Nondegassed, spectroscopic grade toluene and a 10 mm quartz cuvette are used. Dilute solutions ($0.01 < A < 0.05$) are used to minimize reabsorption effects. Quantum yields are determined using eq 1:

$$\Phi_F^{(\text{sample})} = \Phi^{(\text{standard})} \times (\text{Abs}^{(\text{standard})} \times F^{(\text{sample})}) / (\text{Abs}^{(\text{sample})} \times F^{(\text{standard})}) \quad (1)$$

where $\Phi^{(\text{standard})}$ is the reported quantum yield of the standard, Abs is the absorbance at the excitation wavelength, and F is the integrated emission spectra. Fluorescence lifetime is determined on dilute solutions (ca. 10^{-6} M).

Effects on Cell Growth/Viability. MCF-7 (human breast carcinoma) cells are obtained from the Institute of Basic Medical Sciences (IBMS) of the Chinese Academy of Medical Sciences (CAMS). All cell lines are maintained under standard culture conditions (atmosphere of 5% CO_2 and 95% air at 37 °C) in RPMI 1640 medium, supplemented with 10% FBS (fetal calf serum). The cytotoxic effect of **DC-SPC-PPh3** is assessed using the MTT assay. Briefly, the cells in the exponential phase of growth are used in the experimentation. 1.5×10^3 cells/well are seeded onto 96-well plates and allowed to grow for 24 h prior to treatment with **DC-SPC-PPh3**. The incubation time of **DC-SPC-PPh3** is 1−2 h. At the end of this time, the **DC-SPC-PPh3** containing medium is replaced with PBS, MTT is then added to each well (final concentration 0.5 mg/mL) for 4 h at 37 °C, and formazan crystals formed through MTT metabolism by viable cells are dissolved in DMSO. Optical densities are measured at 570 nm. IC_{50} values (concentrations reducing the cell survival fraction by 50%) are obtained by nonlinear regression analysis, using Origin 8.5.

Culture of MCF-7 Cells and Fluorescent Imaging. MCF-7 cells are obtained from the Institute of Basic Medical Sciences (IBMS) of the Chinese Academy of Medical Sciences (CAMS). All cell lines are maintained under standard culture conditions (atmosphere of 5% CO_2 and 95% air at 37 °C) in RPMI 1640 medium, supplemented with 10% FBS (fetal calf serum). MCF-7 cells are grown in the exponential phase of growth on 35 mm glass-bottom culture dishes (Φ 20 mm) for 1−2 days to reach 70−90% confluence. These cells are used in colocalization experimentation. The cells are washed three times with

dx.doi.org/10.1021/jo401379g | J. Org. Chem. 2013, 78, 9153−9160

RPMI 1640, and then are incubated with 2 mL of **DC-SPC-PPh3** (37.5 nM) and Rh-123 (25 nM) in an atmosphere of 5% CO_2 and 95% air at 37 °C. **DC-SPC-PPh3** is first prepared as a DMSO solution with a concentration of 1 mM and is diluted with RPMI 1640 for cell incubation. Cells were washed twice with 1 mL of PBS at rt, and 1 mL of RPMI 1640 culture medium was added and then observed under a confocal microscope (Olympus FV1000).

Single-Molecule Experiments. For the single-molecule experiments, thin-film samples are prepared by spin coating one drop of a dye−polymer−toluene cosolution (10^{-10} M dye, poly[methyl methacrylate] (PMMA), 20 g L^{-1}) at 5000 rpm onto glass microscope coverslips. The resulting thickness of the polymer films amounts to ∼20 nm. The samples are excited with a solid-state laser (MRL-N-656.5, CNI) at 656.5 nm with an excitation intensity of 1.25 kW/cm^2. The output of the laser is directed into a home-built epifluorescence microscope and reflected via a dichroic beam splitter (FF660-Di, Semrock) toward an infinity-corrected oil-immersion objective (UPLSAPO, 100×, NA = 1.4, Olympus). In the plane of the sample, the excitation is defocused to an area of about 40 × 40 mm^2 by an additional lens with long focal distance (f = 300 mm). The emission from the dyes is collected by the objective, passed through the dichroic beam splitter and two dielectric filters (HQ680LP, D680/30, Chroma), and is focused onto the chip of a back-illuminated electron-multiplying charge-coupled device (EMCCD, iXon DV897, Andor Technology). Typically, a fluorescence-microscopy image displays about 30 spatially isolated single molecules within the illuminated area. From this area, 5000 fluorescence-microscopy images are registered successively with an exposure time of 50 ms. The total acquisition time is 250 s. All experiments are carried out at rt.

Photostability. **SPC**, **DC-SPC**, **DPC**, **DC-DPC**, and **Cy5** are dissolved in chloroform at a concentration of 10.0 μM, respectively. The solutions are irradiated under a 500 W iodine−tungsten lamp for 10 h at a distance of 250 mm away. An aqueous solution of sodium nitrite (50.0 g/L) is placed between the samples and the lamp as a light filter (to cut off the light shorter than 400 nm) and heat filter. The photostabilities are expressed in the terms of remaining fluorescence (%) calculated from the changes of fluorescence at the fluorescence maximum before and after irradiation by iodine−tungsten lamp.

2PA Cross-Section Measurements. The investigations of the 2PA were performed with a femtosecond laser system (Coherent, Inc.). The output of a Ti:Sapphire laser (Mira 900-F, tuned to 800 nm, with a repetition rate = 76 MHz, average power ≈ 1.1 W, and pulse duration ≈ 200 fs), pumped by the second harmonic of cw Nd3+:YAG laser (Verdi-10), was regeneratively amplified with a 1 kHz repetition rate (Legend Elite USP) providing ∼100 fs pulses (fwhm) with energy ∼3.6 mJ/pulse. This output at 800 nm was split into two separate beams with average power ∼1.8 W each and pumped into two ultrafast optical parametric amplifiers (OPerA Solo (OPA), Coherent Inc.) with a tuning range 0.24−20 μm, ∼100 fs (fwhm), and pulse energies up to ∼100 μJ. A single laser beam from the first OPA was used for direct 2PA cross-section measurements by the open-aperture Z-scan method.[21]

General Procedure for the Synthesis of BODIPY Derivatives. **DC-BDP** (500 mg, 0.97 mmol) and carbazole aldehyde (0.97 mmol) were refluxed in a mixture of toluene (50 mL), acetic acid (1 mL), and piperidine (1 mL). Any water formed during the reaction was removed azeotropically by heating 8 h in a Dean−Stark apparatus. Crude product was then concentrated under vacuum, and purified by silica gel column chromatography.

SPC. **BDP** (1.11 mmol, 500 mg) and *N*-propargyl-4-carbazole aldehyde (1.11 mmol, 259 mg) were added to a 100 mL round bottomed flask containing 50 mL of toluene, and to this solution were added piperidine (1 mL) and acetic acid (1 mL). The mixture was heated under reflux by using a Dean−Stark trap, and the reaction was monitored by TLC 1:3 CH_2Cl_2:hexanes (R_f 0.3). When all of the starting material had been consumed, the mixture was cooled to rt, and solvent was evaporated. Water (300 mL) added to the residue and the product was extracted into the CH_2Cl_2 (3 × 200 mL). Organic phase was dried over Mg_2SO_4, evaporated, and residue was purified by silica gel column chromatography using 1:3 CH_2Cl_2:hexanes as the eluent, which yielded the desired product **SPC** as a purple powder (255 mg, 35%). mp 258−259 °C. ^{1}H NMR (400 MHz, $CDCl_3$): δ 8.28 (s, 1H), 8.15 (d, J = 7.6 Hz, 1H), 7.85 (d, J = 8.0 Hz, 2H), 7.78 (d, J = 10.0 Hz 3H), 7.72 (d, J = 16.0 Hz, 1H), 7.45−7.52 (m, 4H), 7.31 (t, J = 8.0 Hz, 1H), 7.08 (d, J = 8.0 Hz, 2H), 6.67 (s, 1H), 6.01 (s, 1H), 5.05 (s, 2H), 2.63 (s, 3H), 2.29 (s, 1H), 1.49 (s, 3H), 1.44 (s, 3H). ^{13}C NMR (100 MHz, $CDCl_3$): δ 155, 154, 141, 138, 135, 130, 128, 126, 124, 123, 121, 120, 109, 95, 73, 33, 30, 15. m/z (TOF MS ES): calcd M^+ for $C_{35}H_{27}BN_3F_2NaI$, 688.1209; found, 688.1222.

DC-SPC. **DC-BDP** (0.97 mmol, 500 mg) and *N*-propargyl-4-carbazole aldehyde (0.97 mmol, 225 mg) were added to a 100 mL round bottomed flask containing 50 mL of toluene, and to this solution were added piperidine (1 mL) and acetic acid (1 mL). The mixture was heated under reflux by using a Dean−Stark trap, and the reaction was monitored by TLC 1:3 CH_2Cl_2:hexanes (R_f 0.4). When all of the starting material had been consumed, the mixture was cooled to rt, and solvent was evaporated. Water (300 mL) added to the residue and the product was extracted into the CH_2Cl_2 (3 × 200 mL). Organic phase was dried over Mg_2SO_4, evaporated, and residue was purified by silica gel column chromatography using 1:3 CH_2Cl_2:hexanes as the eluent, which yielded the desired product **DC-SPC** as a blue powder (220 mg, 35%). mp 263−264 °C. ^{1}H NMR (400 MHz, $CDCl_3$): δ 8.31 (s, 1H), 8.27 (s, 1H), 8.16 (d, J = 8.0 Hz, 1H), 7.89 (d, J = 8.0 Hz, 2H), 7.85 (d, J = 8.0 Hz 1H), 7.75 (d, J = 16.0 Hz, 1H), 7.49−7.55 (m, 3H), 7.31 (t, J = 6.0 Hz, 1H), 7.06 (d, J = 8.0 Hz, 2H), 5.07 (s, 2H), 2.66 (s, 3H), 2.30 (s, 1H), 1.46 (s, 3H), 1.42 (s, 3H). ^{13}C NMR (100 MHz, $CDCl_3$): δ 152.0, 148.6, 140.8, 140.3, 138.9, 138.7, 138.6, 136.6, 134.1, 130.5, 130.1, 129.8, 128.8, 126.4, 125.8, 123.9, 123.3, 120.8, 120.3, 115.2, 109.3, 109.1, 95.3, 72.7, 32.6, 12.6, 12.2. m/z (TOF MS ES): calcd M^+ for $C_{35}H_{25}BN_3F_2NaCl_2I$, 756.0429; found, 756.0435.

DPC. **BDP** (1.11 mmol, 500 mg) and *N*-propargyl-4-carbazole aldehyde (3.33 mmol, 777 mg) were added to a 100 mL round bottomed flask containing 50 mL of toluene, and to this solution were added piperidine (1.5 mL) and acetic acid (1.5 mL). The mixture was heated under reflux by using a Dean−Stark trap, and the reaction was monitored by TLC 1:2.5 CH_2Cl_2:hexanes (R_f 0.3). When all of the starting material had been consumed, the mixture was cooled to rt, and solvent was evaporated. Water (300 mL) added to the residue and the product was extracted into the CH_2Cl_2 (3 × 200 mL). Organic phase was dried over Mg_2SO_4, evaporated, and the residue was purified by silica gel column chromatography using 1:2.5 CH_2Cl_2:hexanes as the eluent, which yielded the desired product **DPC** as a green powder (733 mg, 75%). mp 267−269 °C. ^{1}H NMR (400 MHz, THF-d_8): δ 8.36 (s, 2H), 8.22 (d, J = 8.0 Hz, 2H), 7.93 (d, J = 8.0 Hz, 2H), 7.84 (d, J = 7.2 Hz 2H), 7.82 (s, 2H), 7.58−7.65 (m, 6H), 7.47 (t, J = 8.0 Hz, 2H), 7.26 (t, J = 8.0 Hz, 4H), 6.83 (s, 2H), 6.01 (s, 2H), 5.21 (s, 4H), 2.75 (s, 2H), 1.54 (s, 6H). ^{13}C NMR (100 MHz, THF-d_8): δ 151.3, 138.8, 136.4, 129.1, 126.9, 124.1, 118.6, 118.0, 107.6, 107.3, 92.6, 76.1, 70.8, 29.9, 12.3. m/z (TOF MS ES): calcd M^+ for $C_{51}H_{36}BN_4F_2I$, 880.2046; found, 880.2010.

DC-DPC. **DC-BDP** (0.97 mmol, 500 mg) and *N*-propargyl-4-carbazole aldehyde (2.91 mmol, 678 mg) were added to a 100 mL round bottomed flask containing 50 mL of toluene, and to this solution were added piperidine (1.5 mL) and acetic acid (1.5 mL). The mixture was heated under reflux by using a Dean−Stark trap, and the reaction was monitored by TLC 1:2.5 CH_2Cl_2:hexanes (R_f 0.35). When all of the starting material had been consumed, the mixture was cooled to rt, and solvent was evaporated. Water (300 mL) added to the residue and the product was extracted into the CH_2Cl_2 (3 × 200 mL). Organic phase was dried over Mg_2SO_4, evaporated, and residue was purified by silica gel column chromatography using 1:2.5 CH_2Cl_2:hexanes as the eluent, which yielded the desired product **DC-DPC** as a brown powder (728 mg, 80%). mp >300 °C. ^{1}H NMR (400 MHz, $CDCl_3$): δ 8.32 (d, J = 16.0 Hz 1H), 8.18 (d, J = 8.0 Hz, 1H), 7.83−7.93 (m, 3H), 7.52−7.55 (m, 3H), 7.30 (t, J = 6.0 Hz 1H), 7.09 (d, J = 8.0 Hz 1H), 5.07 (s, 2H), 2.64 (s, 3H). ^{13}C NMR: nd. m/z (TOF MS ES): calcd $[M + Na]^+$ for $C_{51}H_{34}BN_4F_2NaCl_2I$, 971.1164; found, 971.1168.

dx.doi.org/10.1021/jo401379g | J. Org. Chem. 2013, 78, 9153−9160

DC-SPC-PPh3. Under a nitrogen atmosphere, $CuSO_4 \cdot 5H_2O$ (2.8 mg, 0.012 mmol) in H_2O (1 mL) and Na-ascorbate (4.2 mg, 0.022 mmol) in H_2O (1 mL) followed by DIPEA (30 mL, 0.174 mmol) were added to a solution of (3-azidopropyl)triphenylphosphonium bromide (45 mg, 0.106 mmol) in EtOH (8 mL). A solution of **DC-SPC** (63 mg, 0.086 mmol) in toluene (20 mL) then was slowly added dropwise to the mixture in the absence of light. The reaction mixture was stirred in the dark for 12 h at rt. Still in the absence of light, the solvent was evaporated off under vacuum, and the product was purified by silica gel column chromatography using 1:35 EtOH:CH_2Cl_2 as the eluent, which yielded the desired product **DC-SPC-PPh3** as a dark blue solid (84.7 mg, 85%). mp 235−236 °C. ^{1}H NMR (400 MHz, $CDCl_3$): δ 8.62 (s, 1H), 8.25−8.13 (m, 3H), 7.89−7.50 (m, 20H), 7.26 (s, 2H), 5.73 (s, 2H), 4.47 (s, 2H), 3.56 (s, 2H), 2.57 (s, 3H), 2.04 (s, 2H), 1.42 (s, 3H), 1.36 (s, 3H). ^{13}C NMR (100 MHz, $CDCl_3$): δ 151.6, 147.7, 143.4, 141.4, 140.9, 140.4, 138.8, 134.0, 133.9, 133.3, 130.8, 130.7, 127.9, 126.9, 124.8, 124.0, 123.5, 122.7, 121.8, 121.2, 120.4, 118.9, 118.0, 111.2, 97.1, 49.7, 49.3, 23.5, 18.9, 18.4, 12.8, 12.3. ^{31}P NMR (100 MHz, DMSO) δ 24. *m*/*z* (TOF MS ES): calcd $[M - Br]^+$ for $C_{56}H_{46}BN_6F_2PCl_2I$, 1079.2005; found, 1079.2042.

■ ASSOCIATED CONTENT

Supporting Information

Polar sensitivity measurements, computational details, ^{1}H and ^{13}C spectra, and structure of **Cy5**. This material is available free of charge via the Internet at http://pubs.acs.org.

■ AUTHOR INFORMATION

Corresponding Authors

*E-mail: xiaoyi@dlut.edu.cn.
*E-mail: jlqu@szu.edu.cn.
*E-mail: belfield@ucf.edu.

Notes

The authors declare no competing financial interest.

■ ACKNOWLEDGMENTS

Y.X. thanks the National Natural Science Foundation of China (nos. 21174022, 21376038), the National Basic Research Program of China (no. 2013CB733702), and the Specialized Research Fund for the Doctoral Program of Higher Education (no. 20110041110009) for financial support. J.Q. thanks the National Natural Science Foundation of China (no. 61078067) and the State Key Laboratory of Fine Chemicals (KF1114) for support. K.D.B. thanks the National Science Foundation (CHE-0840431 and CHE-0832622) for support.

■ REFERENCES

(1) (a) Weissleder, R. *Nat. Biotechnol.* **2001**, *19*, 316−317. (b) Kiyose, K.; Kojima, H.; Nagano, T. *Chem. Asian J.* **2008**, *3*, 506−515.

(2) (a) Peng, X.; Yang, Z.; Wang, J.; Fan, J.; He, Y.; Song, F.; Wang, B.; Sun, S.; Qu, J.; Qi, J.; Yan, M. *J. Am. Chem. Soc.* **2011**, *133*, 6626−6635. (b) Yu, F.; Li, P.; Li, G.; Zhao, G.; Chu, T.; Han, K. *J. Am. Chem. Soc.* **2011**, *133*, 11030−11033. (c) Myochin, T.; Kiyose, K.; Hanaoka, K.; Kojima, H.; Terai, T.; Nagano, T. *J. Am. Chem. Soc.* **2011**, *133*, 3401−3409.

(3) Benson, R. C.; Kues, H. A. *J. Chem. Eng. Data* **1977**, *42*, 379−383.

(4) (a) Fu, M.; Xiao, Y.; Qian, X.; Zhao, D.; Xu, Y. *Chem. Commun.* **2008**, 1780−1782. (b) Koide, Y.; Urano, Y.; Hanaoka, K.; Terai, T.; Nagano, T. *ACS Chem. Biol.* **2011**, *6*, 600−608.

(5) (a) Zhang, X.; Yu, H.; Xiao, Y. *J. Org. Chem.* **2012**, *77*, 669−673. (b) Bellier, Q.; Pégaz, S.; Aronica, C.; Guennic, B. L.; Andraud, C.; Maury, O. *Org. Lett.* **2011**, *13*, 22−25. (c) Loudet, A.; Bandichhor, R.; Wu, L.; Burgess, K. *Tetrahedron* **2008**, *64*, 3642−3654. (d) Loudet, A.; Bandichhor, R.; Burgess, K.; Palma, A.; McDonnell, S. O.; Hall, M. J.; O 'Shea, D. F. *Org. Lett.* **2008**, *10*, 4771−4774.

(6) (a) Yuan, L.; Lin, W.; Yang, Y.; Chen, H. *J. Am. Chem. Soc.* **2012**, *134*, 1200−1211. (b) Ahn, H. Y.; Yao, S.; Wang, X.; Belfield, K. D. *ACS Appl. Mater. Interfaces* **2012**, *4*, 2847−2854.

(7) (a) Buyukcakir, O.; Bozdemir, O. A.; Kolemen, S.; Erbas, S.; Akkaya, E. U. *Org. Lett.* **2009**, *11*, 4644−4647. (b) Bura, T.; Retailleau, P.; Ulrich, G.; Ziessel, R. *J. Org. Chem.* **2011**, *76*, 1109−1117.

(8) (a) Yu, H.; Xiao, Y.; Jin, L. *J. Am. Chem. Soc.* **2012**, *134*, 17486−17489. (b) Dodani, S. C.; Leary, S. C.; Cobine, P. A.; Winge, D. R.; Chang, C. J. *J. Am. Chem. Soc.* **2011**, *133*, 8606−8616. (c) Masanta, G.; Lim, C. S.; Kim, H. J.; Han, J. H.; Kim, H. M.; Cho, B. R. *J. Am. Chem. Soc.* **2011**, *133*, 5698−5700.

(9) (a) Goeb, S.; Ziessel, R. *Org. Lett.* **2007**, *9*, 737−740. (b) Shen, Z.; Röhr, H.; Rurack, K.; Uno, H.; Spieles, M.; Schulz, B.; Reck, G.; Ono, N. *Chem.-Eur. J.* **2004**, *10*, 4853−4871.

(10) (a) Rurack, K.; Kollmannsberger, M.; Daub, J. *Angew. Chem., Int. Ed.* **2001**, *40*, 385−387. (b) Burghart, A.; Kim, H.; Welch, M. B.; Thoresen, L. H.; Reibenspies, J.; Burgess, K.; Bergström, F.; Johansson, L. B.-A. *J. Org. Chem.* **1999**, *64*, 7813−7819. (c) Gorman, A.; Killoran, J.; O'Shea, C.; Kenna, T.; Gallagher, W. M.; O'Shea, D. F. *J. Am. Chem. Soc.* **2004**, *126*, 10619−10631. (d) Yu, Y.; Descalzo, A. B.; Shen, Z.; Röhr, H.; Liu, Q.; Wang, Y.; Spieles, M.; Li, Y.; Rurack, K.; You, X. *Chem. Asian J.* **2006**, *1*−*2*, 176−187.

(11) (a) Zhao, W.; Carreira, E. M. *Angew. Chem., Int. Ed.* **2005**, *44*, 1677−1679. (b) Umezawa, K.; Matsui, A.; Nakamura, Y.; Citterio, D.; Suzuki, K. *Chem.-Eur. J.* **2009**, *15*, 1096−1106.

(12) Baruah, M .; Qin, W.; Flors, C.; Hofkens, J.; Vallee, R. A. L.; Beljonne, D.; Van der Auweraer, M.; De Borggraeve, W. M.; Boens, N. *J. Phys. Chem. A* **2006**, *110*, 5998−6009.

(13) (a) Zhang, D.; Wang, Y.; Xiao, Y.; Qian, S.; Qian, X. *Tetrahedron* **2009**, *65*, 8099−8103. (b) Zhang, D.; Martín, V.; García-Moreno, I.; Costela, A.; Pérez-Ojeda, M. E.; Xiao, Y. *Phys. Chem. Chem. Phys.* **2011**, *13*, 13026−13033.

(14) Deniz, E.; Isbasar, G. C.; Bozdemir, O. A.; Yildirim, L. T.; Siemiarczuk, A.; Akkaya, E. U. *Org. Lett.* **2008**, *10*, 3401−3403.

(15) Loudet, A.; Burgess, K. *Chem. Rev.* **2007**, *107*, 4891−4932.

(16) (a) Helmchen, F.; Denk, W. *Nat. Methods* **2005**, *2*, 932−940. (b) Zipfel, W. R.; Williams, R. M.; Webb, W. W. *Nat. Biotechnol.* **2003**, *21*, 1369−1377. (c) Kim, H. M.; Cho, B. R. *Acc. Chem. Res.* **2009**, *42*, 863−872. (d) Kim, H. M.; Cho, B. R. *Chem. Asian J.* **2011**, *6*, 58−69.

(17) (a) Rihn, S.; Retailleau, P.; Bugsaliewicz, N.; Nicola, A. D.; Ziessel, R. *Tetrahedron Lett.* **2009**, *50*, 7008−7013. (b) Han, F.; Chi, L.; Liang, X.; Ji, S.; Liu, S.; Zhou, F.; Wu, Y.; Han, K.; Zhao, J.; James, T. D. *J. Org. Chem.* **2009**, *74*, 1333−1336.

(18) (a) Lakowicz, J. R. *Principles of Fluorescence Spectroscopy*, 2nd ed.; Kluwer Academic/Plenum Publishers: New York, 1999. (b) Valeur, B. *Molecular Fluorescence: Principles and Applications*; Wiley-VCH Verlag: GmbH, 2001. (c) Parson, W. W. *Modern Optical Spectroscopy: With Examples from Biophysics and Biochemistry*; Springer-Verlag: Berlin Heidelberg, 2007.

(19) (a) Heilemann, M.; Margeat, E.; Kasper, R.; Sauer, M.; Tinnefeld, P. *J. Am. Chem. Soc.* **2005**, *127*, 3801−3806. (b) Cordes, T.; Vogelsang, J.; Anaya, M.; Spagnuolo, C.; Gietl, A.; Summerer, W.; Herrmann, A.; Müllen, K.; Tinnefeld, P. *J. Am. Chem. Soc.* **2010**, *132*, 2404−2409. (c) Haase, M.; Hübner, C. G.; Nolde, F.; Müllen, K.; Basché, T. *Phys. Chem. Chem. Phys.* **2011**, *13*, 1776−1785.

(20) (a) Chalmers, S.; Caldwell, S. T.; Quin, C.; Prime, T. A.; James, A. M.; Cairns, A. G.; Murphy, M. P.; McCarron, J. G.; Hartley, R. C. *J. Am. Chem. Soc.* **2012**, *134*, 758−761. (b) Dickinson, B. C.; Chang, C. J. *J. Am. Chem. Soc.* **2008**, *130*, 9638−9639.

(21) Belfield, K. D.; Bondar, M. V.; Morales, A. R.; Yue, X.; Luchita, G.; Przhonska, O. V.; Kachkovsky, O. D. *ChemPhysChem* **2012**, *13*, 3481−3491.